Modifying of surface properties and structural characteristics of low energy argon beam irradiated methylcellulose/TiO_2 nanocomposite films

R. Altuijri[a], A. Atta[b,*], E. Abdeltwab[b], M. M. Abdelhamied[c]
[a]*Department of Physics, College of Science, Princess Nourah bint Abdulrahman University, P.O. Box 84428, Riyadh 11671, Saudi Arabia*
[b]*Physics Department, College of Science, Jouf University, P.O. Box: 2014, Sakaka, Saudi Arabia*
[c]*Charged Particles Lab., Radiation Physics Department, National Center for Radiation Research and Technology (NCRRT), Egyptian Atomic Energy Authority (EAEA), Cairo, Egypt*

Flexible polymeric nanocomposites MC/TiO_2 films, which consisting of titanium dioxide (TiO_2) and methyl cellulose (MC) were fabricated in this research for applied in coating devices. The successful manufacturing of MC/TiO_2 sheets were verified by FTIR, SEM and XRD methods, which demonstrated a uniform distribution of TiO_2 in MC. Additionally, the chemical bonds of MC and TiO_2 contribute for the broadening and decreasing of MC in the peaks intensity of XRD and FTIR with increasing TiO_2, indicating the successful incorporation of TiO_2 in MC. The impacts of argon beam bombardment on MC/TiO_2 composites using cold cathode source with fluencies (2.5×10^{15}, 5×10^{15} and 7.5×10^{15} ions/cm^2). The contact angle, work of adhesion and surface free energy of MC/TiO_2 were determined as a function of ion irradiation. The water contact angle is decreased from 70.32^o to 43.34^o by increasing ion fluence from 2.5×10^{15} ions/cm^2 to 7.5×10^{15} ions/cm^2, while the surface free energy is enhanced from 38.83 mJ/m^2 to 64.17 mJ/m^2. The collected data confirmed that the surface wettability of the irradiated MC/TiO_2 films were improved to be can usage in coating and printing applications.

(Received April 12, 2024; Accepted July 10, 2024)

Keywords: Fabrication, Characterization, Surface properties, Structural

1. Introduction

Recently, many researchers have become attracted to polymer composites because of their intriguing and distinct characteristics as well as the prospective uses they may have in current technological and industrial processes [1, 2]. Due to its special properties, including geometry, light weight, and cost effectiveness, polymer composite materials are becoming more popular [3]. The structure, mechanical attributes, and electrical characteristics of electronic devices have drawn a lot of interest in the field of polymer composites [4]. In addition, scientists are working to create composite films with superior properties for usage in other fields such microelectronics, bioelectronics, and diodes [5]. Biosensors and optical electronics frequently employ composites made of conductive polymers and nanoscale conductive fillers.

Methylcellulose is published in using, because it is easy to use, requires little energy, is inexpensive, and has an environmentally favorable procedure [6]. Water soluble and generated from long-chain cellulose, methylcellulose (MC) has many good qualities [7]. Depending on the level of substitution, MC has an extensive variety of uses because of its excellent characteristics [8]. Methylcellulose is regarded as significant characteristics of viscosity, and surface adherence of nanocomposite materials [9]. One semiconductor material that is already well-known for its unique chemical, optical, and electrical characteristics is titanium dioxide (TiO_2) [11]. TiO_2 has been effectively applied to gas sensors, solar cells, and electrochromic devices [12]. TiO_2-based nanoparticles that are simple to utilize in photoelectrochemical reactions [13]. Typically, the TiO_2

* Corresponding author: aamahmad@ju.edu.sa
https://doi.org/10.15251/DJNB.2024.193.1053

nanoparticles are immobilized on a variety of surfaces, including quartz, silica, alumina, and glass [14, 15].

Surface characteristics would be improved by exposed to ion irradiation to the polymer composite [16]. The composite structure, as well as the shape and interfacial properties of each individual counterpart, determine the properties of the nanocomposite [17]. Improving the properties of the polymer composites is a result outcome of surface modifications that induced by ion beam irradiation [18]. Certain types of radicals are produced during ion beam treatment. Ion beam-treated polymer composites modify their electrical conductivity and surface characteristics to make them more useful for optoelectronic devices [19]. One way to make polymer composites more biocompatible is to modify their surface wettability using ion irradiation methods [20].

The main goal in this work is to create a novel polymer composite by including TiO_2 into the MC. In this work, the MC/TiO_2 composite were successful preparation using the chemical solution casting method. Then the films were characterized using different techniques as SEM, FTIR and XRD analyses, and then exposed these samples for ion beam by using environmentally friendly cold cathode ion source. The impacts of argon beam on the surface properties of MC/TiO_2 will be studied to direct these irradiated samples for used in different applications as coating, printing and supercapacitors

2. Experimental work

For the chemicals, Methylcellulose (MC, MW~ 680 gm/mol), titanium dioxide nanopowder (TiO_2, 99.6%), Distilled water (99.5%) and ethanol (99.6%) were purchased from Sigma-Aldrich. The method of solution casting was applied to prepare the MC/TiO_2 films, which was discussed before [21, 22]. For preparation the MC solution, the MC was dissolved in a mixture of solvents (distilled water and ethanol). At room temperature, continuous magnet stirrer was used for 4 h until the MC powder completely dissolved in solvent. The pure MC film (pristine) were manufactured by pouring the polymer solutions in a petri dishes. At 40^o C. For synthesis the composite films of MC/TiO_2, 0.25 g of TiO_2 dissolved in 30 mL of deionized water using the continuous stirring. Three different ratio of TiO_2 solution (2%, 4%, and 6%) were introduced to the same amount of MC solution (10 ml). After that, these solutions continuously magnetic stirred for getting a homogeneous mixture of MC/TiO_2. Finally, the resultant mixtures of MC/TiO_2 were casted in a petri dishes, then left in air for three days to dry.

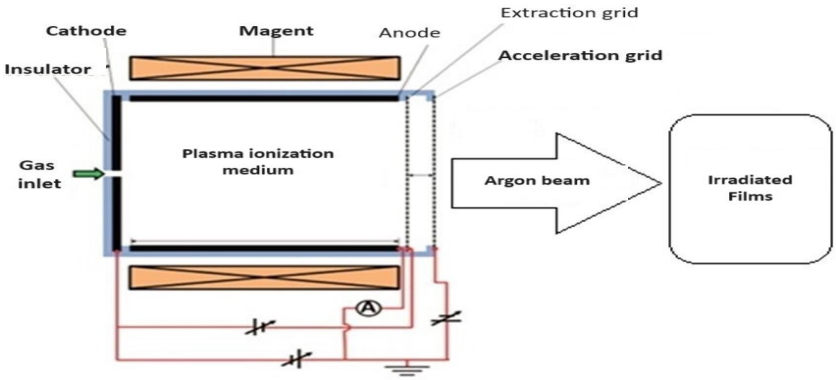

Fig. 1. A broad beam cold cathode ion source.

At fluencies of 2.5x10^{15}, 5.0x10^{15}, and 7.5x10^{15} ions/cm^2, the MC/TiO_2 film is subjected to an argon beam ion source, as shown in Figure 1. As mentioned earlier, the ionization and extraction regions are the two primary components of the ion source [23]. At a pressure of 1.6x10^{-4} mbar, a beam intensity of 130 □A/cm^2, and an energy of 4 keV, the extraction system was used to finally

extract the ion beam. The structure characterization of the pristine and MC/TiO_2 was carried out by XRD with λ = 1.5406 Å of 2θ = 4 º to 80º. The FTIR (Shimadzu FTIR-340 , USA) of the pristine and composite films were revealed in the wavenumber 400 cm^{-1} to 4000 cm^{-1}. The surface morphology analysis of all films was performed employing the SEM (Hitachi, Japan). The surface free energies were determined by measuring the contact angles with two liquids: diiodomethane and distilled water. Using the (TRIM/SRIM) simulation program, the changes in structure caused by argon irradiation of MC/TiO_2 are theoretically studied [24].

3. Results and discussion

Figure 2 depicts the XRD data of the pure MC and MC/TiO_2 films with varying amounts of TiO_2. The XRD revealed the semi crystalline structure of the pure MC. In which, the patterns two strong peaks around 2θ = 8.09º and 2θ=20.8º which assigned to the glucose-type crystalline order in the MC and the intermolecular structure of MC matrix. In addition, the pattern also presented another reflection which seems as broad hump around 2θ =13.55º due to a more hydrated structure of the pure film [25]. On the other hand, the patterns of nanocomposite films have new diffraction peaks otherwise the MC peaks. In which, these peaks reveal the majority as rutile phase (R phase) and a little amount of anatase phase (A phase) of TiO_2. Especially, the diffraction peaks of the rutile TiO_2 located at 2θ = 27.28°, 36.01°, 39.04, 41.14°, 44.06°, 54.35°, 56.57°, 62.82°, 64.17°, and 69.05° which are assigned to the (110), (101), (200), (111), (210), (211), (220), (002), (310), and (112) planes [26]. Further, the reflection peaks of anatase TiO_2 placed around 2θ ~ 25.45° and 37.57° are corresponded to the (101) and (004) reticular planes [27].

In addition, one can be observed that the increase in amounts of TiO_2, which are dispersed in MC matrix only led to the increase in intensity of TiO_2 peaks, which confirm that there is no change on the structure of TiO_2. Hence, these information's reveal the successful introducing of TiO_2 NPs into MC matrix. For MC peaks, their position were shifted and their intensity gradually decreased with increasing the contents of TiO_2, which provide the incorporation of TiO_2 into MC structure and the two materials interacted at the molecular scale. These results show that the amorphicity of MC increased with increasing the concentrations of TiO_2, which is useful for increasing the properties of MC due to increasing the defects state [28].

The Scherrer expression in equation (1) was used to determine the average crystallite size for the main peak at 2θ ~ 27.28° of the three TiO_2 samples (listed in Table 1) [29, 30]:

$$L = \frac{0.89\,\lambda}{\beta\ COS\theta} \tag{1}$$

where L refers to the particle diameter, λ represents the X-ray wavelengths (1.54 Å), β is related to broadening. It is obvious that the crystallite size of TiO_2 increases with increasing the ratio of NPs to be 17.43 nm, 23.54 nm, and 35.58 nm of the MC/2%TiO_2, MC/4%TiO_2 and MC/6%TiO_2, respectively. Moreover, the particle diameter (R) for TiO_2 NPs is deduced by [31]:

$$\mathrm{R} = \frac{\lambda}{\sin\beta\cos 2\theta} \tag{2}$$

It is found that the particle diameter for TiO_2 of the MC/2%TiO_2 is 1.2 μm, which increased to 1.7 and 2.5 μm for the MC/4%TiO_2 and the MC/6%TiO_2. The lattice strain (ε) of the MC/2%TiO_2, MC/4%TiO_2, and MC/6%TiO_2 films was determine using [32]:

$$\varepsilon = \frac{\beta}{4\tan\theta} \tag{3}$$

It can be seen that the addition of higher amounts of TiO_2 NPs reduces the lattice strain, wich reveals the reduction in the crystal lattices with increasing the contents of TiO_2.

Table 1. Values of D, R and ε for TiO_2 NPs of the MC/TiO_2 films.

	(D) (nm)	(R) (μm)	ε x10^{-3}
MC/2%TiO_2	17.43	1.2	8.4
MC/4%TiO_2	23.54	1.7	6.1
MC/6%TiO_2	35.58	2.5	4.1

Figure 3 presents the obtained FTIR absorption spectra of the pristine MC and that loaded with 2, 4, and 6 wt% TiO_2 NPs. The spectrum of the pristine MC has two main characteristic peaks; the first around 3444 cm^{-1} which is caused owing to the stretching vibrations of methylcellulose hydroxyl groups [33, 34]. The second band around 2927 cm^{-1} represented the stretching of the C–H bond [35]. Further, the MC spectrum displays strong band around the position 1059 cm^{-1} is related to the C-O group stretching vibration. The bands at 1646 cm^{-1} and 1187 cm^{-1} are attributed to the C-O carbonyl stretching for the glucose in the cellulose and C-O stretching, respectively [36].

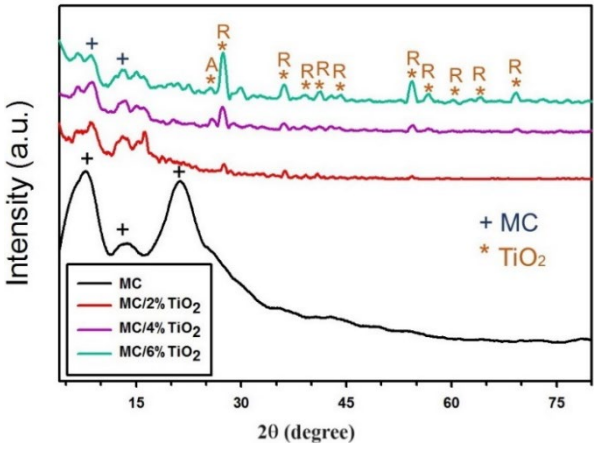

Fig. 2. XRD of the MC, MC/2%TiO_2 MC/4%TiO_2 and MC/6%TiO_2.

The peak around 1374 cm^{-1} and 1462 cm^{-1} of the C-H bending of methyl and methylene groups, respectively [37]. The ring stretching around 947 cm^{-1} confirmed the -OCH_3 groups. As seen from Figure 3, the FTIR bands of TiO_2-doped MC were not varied drastically from those pristine MC film, which reveals that MC films is not damaged after addition the TiO_2 NPs.

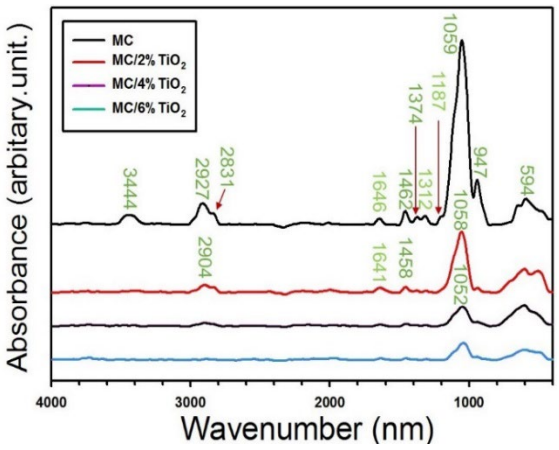

Fig. 3. FTIR of the MC, MC/2%TiO_2 MC/4%TiO_2 and MC/6%TiO_2.

However, one can be observed that the absorbance peaks display a regular decrease in the intensity after loading the TiO_2 particle. Also, the addition of TiO_2 led to a shifting in peaks position. The strong peak at 1059 cm^{-1} for the pristine MC shifted to 1058 cm^{-1} for the MC/2%TiO_2 hybrids and 1052 cm^{-1} for the MC/4%TiO_2 hybrid. Meanwhile, the peak at 1646 cm-1 slightly shifted by ~5 cm^{-1} for the MC/2%TiO_2 hybrids and the peak at 2927 cm^{-1} shifted by 23 cm^{-1} to 2904 cm^{-1}.

The change in microstructure of sample has a great effect on its physical properties. Therefore, the SEM also performed to reveal the microstructure and morphology of the pristine and nanocomposite films. Figure 4 displays the SEM images of the pristine MC, MC/TiO_2-I, and MC/TiO_2-III nanocomposite. One can be seen the significant differences in morphological and microstructure between the pristine MC and nanocomposite films [38]. As shown in Figure 4a, the homogeneous and uniform surface morphology without holes and cracks has been noticed in the pristine MC film. Depending on the concentration of TiO_2 NPs in the MC polymer, granule and many aggregates on the surface of MC/TiO_2-I was appeared as depicted in Figure 4b. This refers to that TiO_2 create aggregates and dispersed into MC matrix. Moreover, the roughness, whiteness, and dispersion increase with TiO_2 as displayed in Figure 4c. [39]

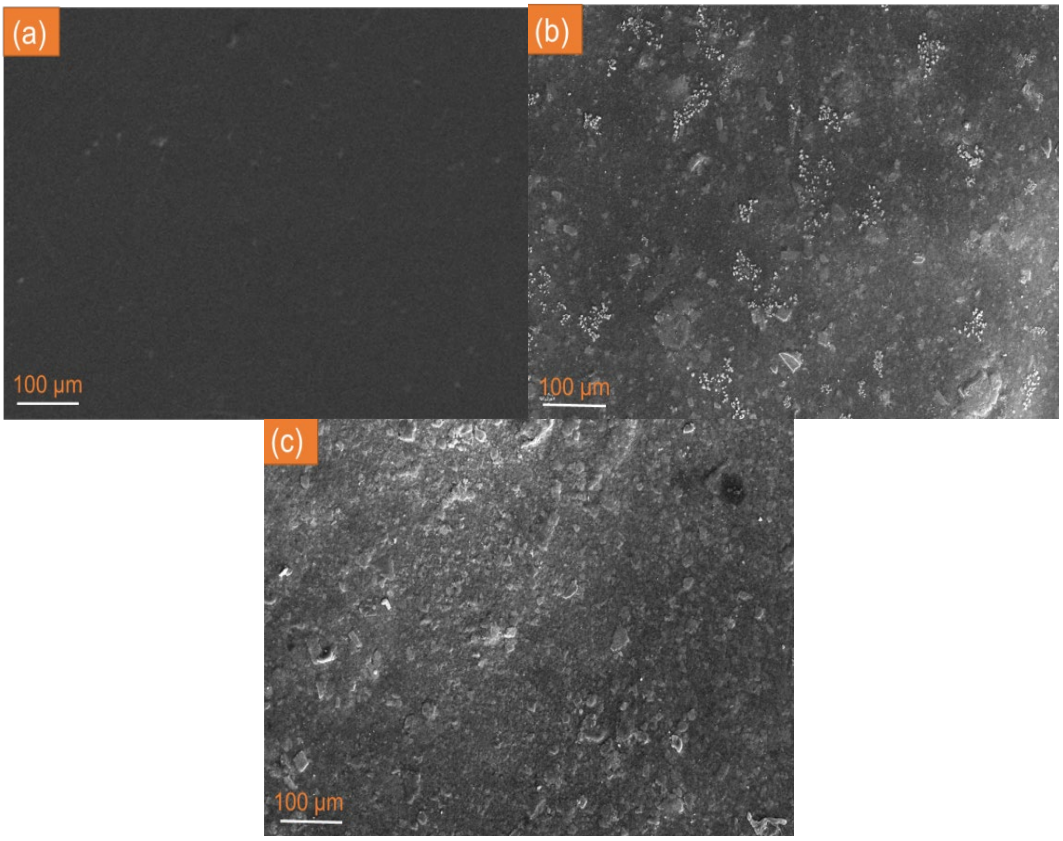

Fig. 4. SEM images of (a) Pristine MC, (b) MC/TiO_2-I, and (C) MC/TiO_2-III films.

The simulation outcomes of 3 kev argon ions reacting with MC/TiO_2 surfaces are shown in Figure 5 of the SRIM/TRIM data collection. Interactions between atoms and molecules in the surface MC/TiO_2 cause the incoming beam to lose energy and accelerate as it collides with the material. Ions encounter carbon, hydrogen, and oxygen atoms upon impact with the MC/TiO_2 surface. Atoms with a lower size can go deeper into a substance with less nuclear displacements [40]. The recoiled particles collide with the target atoms because the ion energy moves them apart, as shown in Figure 5a. The figure shows the ion path value in the composite MC/TiO_2 is about 9.3 nm. Due to the collisions of argon ion with the composite, then a tree of argon ions distributed in MC/TiO_2 with a 1000 Å depth is given in Figure 5b. The ionization caused by ions striking with

surfaces is shown in Figure 5c. The target is significantly more ionized by recoil atoms than by penetrating argon ions.

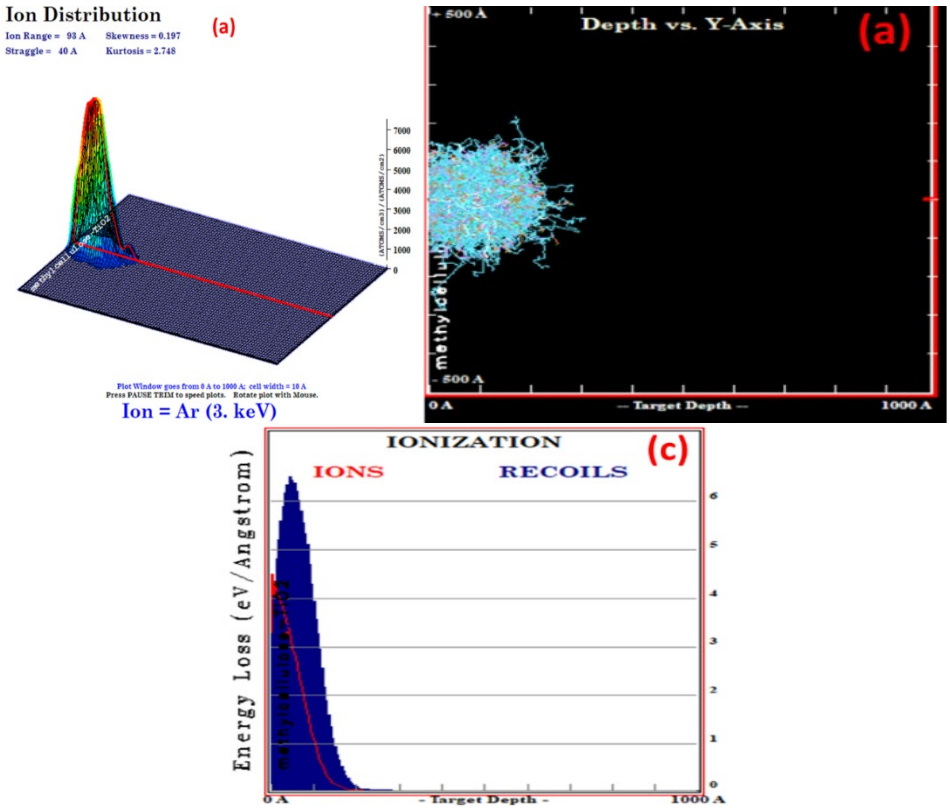

Fig. 5. (a) Argon ions range interacting with MC/TiO_2, (b) tree of argon collision ions in MC/TiO_2, (c) Ionization effects of collided argon beam with MC/TiO_2.

Figure 6 shows the relationship between ion irradiation and the changes in the contact angle of MC/TiO_2 using water and diiodomethane as two separate liquids. The contact angle seems to be getting smaller with increasing ion beam exposure. Figure 6 shows that changing the ion fluence from 2.5x10^{15} ions/cm^2 to 7.5x10^{15} ions/cm^2 reduces the water contact angle from 70.32° to 43.34°, while diiodomethane's contact angle drops from 63.64° to 32.57°.

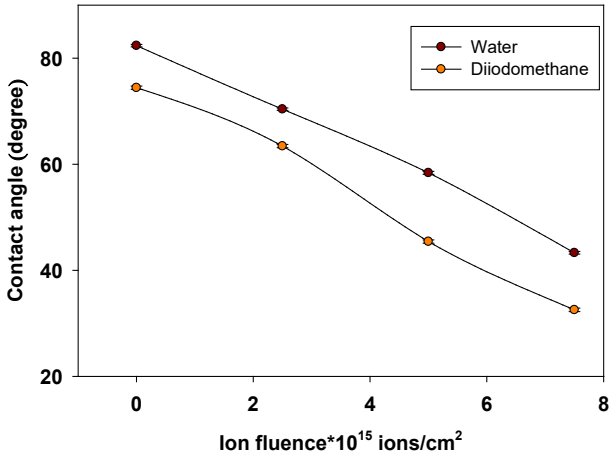

Fig. 6. The contact angle for pure and irradiated MC/TiO_2 films.

The contact angle for all films exposed to ion beam radiation reduces following irradiation, suggesting that the surface becomes more hydrophilic.

Across an interface, the energy of attraction between molecules is represented by the adhesion work, W_a, as a function of the contact angle is given by [41].

$$W_a = \gamma_l(1 + cos\theta) \tag{4}$$

where, γ_l is the surface free energy of liquid, and is θ the contac angle. The variation of the adhesion force of MC/TiO_2 with ion exousre is shown in Figure 7. The W_a is enhanced from 96.28 mJ/m^2 to 124.62 mJ/m^2 for water liquid, where for diiodomethane is enhanced from 73.53 to 93.62 mJ/m^2 by enhancing ion fluence from 2.5x10^{15} ions/cm^2 to 7.5x10^{15} ions/cm^2. It is possible that the increased adhesion work is due to the cleaning of the polymer surface following ion irradiation, as compared to the surface that was not irradiated [42].

Table 2. The contact angle and work of adhesion for MC/TiO_2 at different ion fluencies.

The samples	Contact angle (degree)		Work of adhesion (mJ/m^2)	
	Water	Diiodomethane	Water	Diiodomethane
MC/TiO_2	82.41	74.42	81.68	64.44
2.5×10^{15} ions/cm^2	70.32	63.64	96.28	73.53
5.0×10^{15} ions/cm^2	58.55	45.46	109.98	86.45
7.5×10^{15} ions/cm^2	43.34	32.57	124.62	93.62

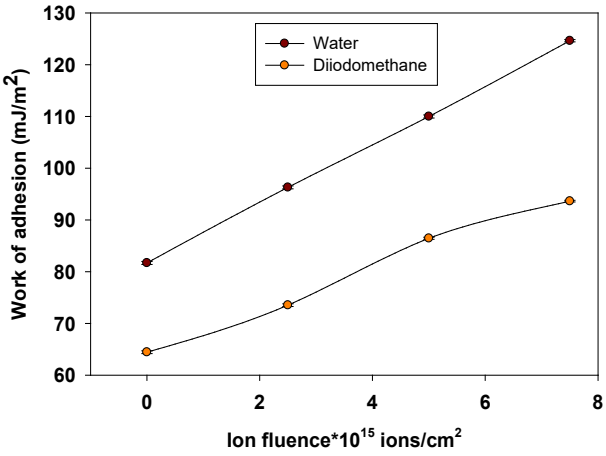

Fig. 7. The work of adhesion for pure and irradiated MC/TiO_2 films.

Using measurements of contact angles and the equations of Young's equation, we were able to predict the surface energy [43]

$$\frac{\gamma_l(1+\cos\theta)}{2\sqrt{\gamma_l^d}} = \sqrt{\gamma_s^d} + \sqrt{\gamma_s^p}\cdot\sqrt{\frac{\gamma_l^p}{\gamma_l^d}} \tag{5}$$

where, the γ_s is surface tensions of solid vapor, γ_{sl} is for solid-liquid, and γ_l is for liquid-vapor, The Equation (5) contains two unknowns dispersive (γ_s^d) and polar (γ_s^p) surface energies of the solid. It is necessary to measure the contact angles of two or more distinct liquids in order to derive these unknown characteristics. The relationship between the surface free energy and the ion beam fluence

is seen in Figure 8. The total surface free energy γ^{st} went up from 38.83 mJ/m^2 to 64.17 mJ/m^2 as a result of increasing the ion fluence from 2.5x10^{15} ions/cm^2 to 7.5x10^{15} ions/cm^2, as demonstrated in Table 3, while the dispersive energy went up from 26.69 mJ/m^2 to 43.78 mJ/m^2. There seems to be a direct correlation between the ion beam fluence and the activation of the composite surface [44].

Table 3. The dispersive, polar, and total surface energies for pure and irradiated MC/TiO$_2$ films.

The samples	Polar γ_s^p (mJ/m^2)	Dispersive γ_s^d (mJ/m^2)	Total γ_s^t (mJ/m^2)
MC/TiO$_2$	8.19	20.43	28.62
2.5×10^{15} ions/cm^2	12.14	26.69	38.83
5.0×10^{15} ions/cm^2	14.32	36.71	51.03
7.5×10^{15} ions/cm^2	20.39	43.78	64.17

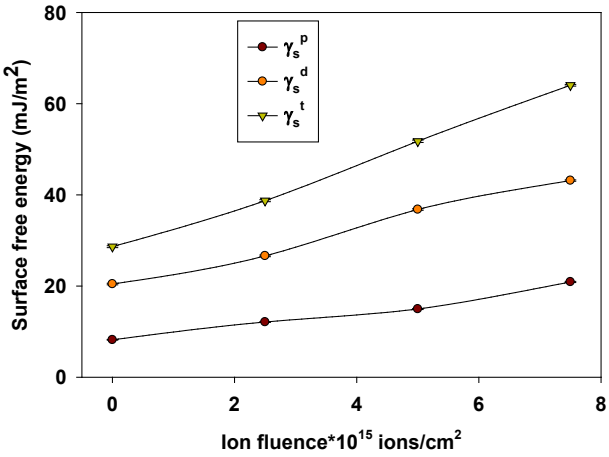

Fig. 8. Polar, dispersive and total free energy for pure and irradiated MC/TiO$_2$ films.

4. Conclusions

The goal of this research is to develop and evaluate novel conductor polymeric composite films. By employing the solution cast technique, the MC/TiO$_2$ composite films were effectively manufactured. The production of the MC and MC/TiO$_2$ nanocomposite films is demonstrated by the XRD, SEM, and FTIR. Imaging microscopy revealed that the incorporation of TiO$_2$ nanoparticles altered the MC morphology. Finding the value of the contact angle allowed us to estimate the surface energy and the work of adhesion. For a water-based liquid, raising the argon ion beam from 2.5x10^{15} ions/cm^2 to 7.5x10^{15} ions/cm^2 raises the adhesion work from 96.28 mJ/m^2 to 124.62 mJ/m^2. By enhancing its hydrophilicity and surface polarity, ion beams also increased the surface energy of MC/TiO$_2$. Depending on the irradiation fluence, the composites surface wettability qualities are improved after ion beam exposure. The irradiated MC/TiO$_2$ composite offers a wide range of applications such a microelectronic devices.

Acknowledgements

Princess Nourah bint Abdulrahman University Researchers Supporting Project number (PNURSP2024R399), Princess Nourah bint Abdulrahman University, Riyadh, Saudi Arabia.

References

[1] Althubiti, N. A., Al-Harbi, N., Sendi, R. K., Atta, A., Henaish, A. M. (2023), Inorganics, 11(2), 74; https://doi.org/10.3390/inorganics11020074

[2] Chen, Y., Xiang, Z., Wang, D., Kang, J., & Qi, H. (2020), RSC advances, 10(40), 23936-23943; https://doi.org/10.1039/D0RA04509H

[3] Atta, A., Negm, H., Abdeltwab, E., Rabia, M., & Abdelhamied, M. M. (2023), Polymers for Advanced Technologies; https://doi.org/10.1002/pat.5997

[4] Atta, A., Abdelhamied, M. M., Abdelreheem, A. M., Althubiti, N. A. (2022), Inorganic Chemistry Communications, 135, 109085; https://doi.org/10.1016/j.inoche.2021.109085

[5] Rathod, S. G., Bhajantri, R. F., Ravindrachary, V., Sheela, T., Pujari, P. K., Naik, J., Poojary, B. (2015), Journal of Polymer Research, 22, 1-14; https://doi.org/10.1007/s10965-015-0657-y

[6] M. M. Abdelhamied, A. Atta, A. Abdelreheem, A. Farag, M. El Okr, Journal of Materials Science: Materials in Electronics 31 (2020) 22629-22641; https://doi.org/10.1007/s10854-020-04774-w

[7] Atta, A., Negm, H., Abdeltwab, E., Rabia, M., Abdelhamied, M. M. (2023), Polymers for Advanced Technologies; https://doi.org/10.1002/pat.5997

[8] Atta, A., Alotaibi, B. M., & Abdelhamied, M. M. (2022), Inorganic Chemistry Communications, 141, 109502; https://doi.org/10.1016/j.inoche.2022.109502

[9] Althubiti, N. A., Al-Harbi, N., Sendi, R. K., Atta, A., Henaish, A. M. (2023), Inorganics, 11(2), 74; https://doi.org/10.3390/inorganics11020074

[10] Abdelhamied, M. M., Atta, A., Abdelreheem, A. M., Farag, A. T. M., El Okr, M. M. (2020), Journal of Materials Science: Materials in Electronics, 31, 22629-22641; https://doi.org/10.1007/s10854-020-04774-w

[11] Althubiti, N. A., Atta, A., Alotaibi, B. M., Abdelhamied, M. M. (2022), Surface Innovations, 11(1-3), 90-100; https://doi.org/10.1680/jsuin.22.00010

[12] Atta, A., Abdelhamied, M. M., Abdelreheem, A. M., Berber, M. R. (2021), Polymers, 13(8), 1225; https://doi.org/10.3390/polym13081225

[13] Abdelhamied, M. M., Abdelreheem, A. M., Atta, A. (2021), Plastics, Rubber and Composites, 1-1; https://doi.org/10.1080/14658011.2021.1928998

[14] Sayed, M., Khan, J. A., Shah, L. A., Shah, N. S., Shah, F., Khan, H. M., Arandiyan, H. (2018), Journal of Physical Chemistry C, 122(1), 406-421; https://doi.org/10.1021/acs.jpcc.7b09169

[15] Goswami, A., Bajpai, A. K., Bajpai, J., Sinha, B. K. (2018), Polymer Bulletin, 75(2), 781-807; https://doi.org/10.1007/s00289-017-2067-2

[16]Fawzy, Y. H. A., Abdel-Hamid, H. M., El-Okr, M. M., Atta, A. (2018), Surface Review and Letters, 25(03), 1850066; https://doi.org/10.1142/S0218625X1850066X

[17]Atta, A., Alotaibi, B. M., & Abdelhamied, M. M. (2022), Inorganic Chemistry Communications, 141, 109502; https://doi.org/10.1016/j.inoche.2022.109502

[18] Althubiti, N. A., Atta, A., Al-Harbi, N., Sendi, R. K., Abdelhamied, M. M. (2023), Optical and Quantum Electronics, 55(4), 348; https://doi.org/10.1007/s11082-023-04600-7

[19] Alotaibi, B. M., Atta, A., Atta, M. R., Abdeltwab, E., Abdel-Hamid, M. M. (2023), Surface Innovations, 1-12; https://doi.org/10.1680/jsuin.22.01078

[20] Alotaibi, B. M., Atta, M. R., Abdeltwab, E., Atta, A., Abdel-Hamid, M. M. (2023), Surface Innovations, 1-11; https://doi.org/10.1680/jsuin.22.01089

[21] Althubiti, N. A., Abdelhamied, M. M., Abdelreheem, A. M., Atta, A. (2022), Inorganic Chemistry Communications, 137, 109229; https://doi.org/10.1016/j.inoche.2022.109229

[22] Abdelhamied, M. M., Atta, A., Alotaibi, B. M., Al-Harbi, N., Henaish, A. M. A., Rabia, M. (2023), Inorganic Chemistry Communications, 157, 111245; https://doi.org/10.1016/j.inoche.2023.111245

[23] Atta A, Abdel-Hamid HM, Fawzy YHA, El-Okr MM (2019), Emerging Materials Research 8(3):354-359; https://doi.org/10.1680/jemmr.19.00054

[24] Ziegler JF, Ziegler MD, Biersack JP (2010), Nuclear Instruments and Methods in Physics Research Section B: Beam Interactions with Materials and Atoms 268(11-12): 1818-1823; https://doi.org/10.1016/j.nimb.2010.02.091

[25] Quiroz, M. T., Lecot, J., Bertola, N., Pinotti, A. (2013), Materials Science and Engineering: C, 33(5), 2918-2925; https://doi.org/10.1016/j.msec.2013.03.021

[26] Du, J., Sun, H. (2014), ACS applied materials & interfaces, 6(16), 13535-13541; https://doi.org/10.1021/am502663j

[27] Govindasamy, G., Murugasen, P., Sagadevan, S. (2016), Materials Research, 19, 413-419; https://doi.org/10.1590/1980-5373-MR-2015-0411

[28] Atta, A., Abdelhamied, M. M., Abdelreheem, A. M., Althubiti, N. A. (2022), Inorganic Chemistry Communications, 135, 109085; https://doi.org/10.1016/j.inoche.2021.109085

[29] Maleky, S., Asadipour, A., Nasiri, A., Luque, R., Faraji, M. (2022), Journal of Polymers and the Environment, 30(8), 3351-3367; https://doi.org/10.1007/s10924-022-02428-y

[30] Abdelhamied, M. M., Gao, Y., Li, X., Liu, W. (2022), Applied Physics A, 128(1), 57; https://doi.org/10.1007/s00339-021-05189-y

[31] Rajendran, S., Sivakumar, M., Subadevi, R. (2004), Materials letters, 58(5), 641-649; https://doi.org/10.1016/S0167-577X(03)00585-8

[32] Cardoso, G. V., Di Salvo Mello, L. R., Zanatta, P., Cava, S., Raubach, C. W., Moreira, M. L. (2018), Cellulose, 25, 2331-2341; https://doi.org/10.1007/s10570-018-1734-2

[33] El-Sayed, S., Abel-Baset, T., Abou Elfadl, A., Hassen, A. (2015), Physica B: Condensed Matter, 464, 17-27; https://doi.org/10.1016/j.physb.2015.02.016

[34] Horikawa, Y., Itoh, T., Sugiyama, J. (2006), Cellulose, 13, 309-316; https://doi.org/10.1007/s10570-005-9037-9

[35] Maleky, S., Asadipour, A., Nasiri, A., Luque, R., Faraji, M. (2022), Journal of Polymers and the Environment, 30(8), 3351-3367; https://doi.org/10.1007/s10924-022-02428-y

[36] Barud, H. D. S., Assunção, R. M. N., Martines, M. A. U., Dexpert-Ghys, J., Marques, R. F. C., Messaddeq, Y., Ribeiro, S. J. L. (2008), Journal of Sol-Gel Science and Technology, 46, 363-367; https://doi.org/10.1007/s10971-007-1669-9

[37] Rangelova, N., Radev, L., Nenkova, S., Miranda Salvado, I. M., Vas Fernandes, M. H., Herzog, M. (2011), Central European Journal of Chemistry, 9, 112-118; https://doi.org/10.2478/s11532-010-0123-y

[38] Amin, G. A. M., Abd-El Salam, M. H. (2014), Materials Research Express, 1(2), 025024; https://doi.org/10.1088/2053-1591/1/2/025024

[39]A. Atta, Surface Innovations 9 (2020) 17-24; https://doi.org/10.1680/jsuin.20.00020

[40]Abdeltwab, E., Atta, A. (2021), Surface Innovations, 40, 1-9.

[41] Papakonstantinou, D., Amanatides, E., Mataras, D., Ioannidis, V., Nikolopoulos, P. (2007), Plasma Processes and Polymers, 4(S1), S1057-S1062; https://doi.org/10.1002/ppap.200732405

[42]-Abdeltwab, E., Atta, A. (2022), ECS Journal of Solid State Science and Technology, 11(4), 043012; https://doi.org/10.1149/2162-8777/ac66fe

[43]-Owens, D. K., Wendt, R. C. (1969), Journal of applied polymer science, 13(8), 1741-1747; https://doi.org/10.1002/app.1969.070130815

[44] Atta, A., Abdeltwab, E. (2022), Brazilian Journal of Physics, 52(1), 1-10; https://doi.org/10.1007/s13538-021-01011-5